Article | Received 9 October 2024; Accepted 25 November 2024; Published 29 November 2024
https://doi.org/10.55092/bm20240010

The spatial orientation of histidine via five-armed alkylamino siloxane improved the properties of the cationic gene delivery vector

Viola B. Morris[1,2,*] and Chandra P. Sharma[1,*]

[1] Division of Biosurface technology, Biomedical Technology Wing, Sree Chitra Tirunal Institute for Medical Science and Technology, Thiruvananthapuram, India
[2] Department of Medicine, Division of Cardiology, Emory University School of Medicine, Atlanta, GA, USA

* Correspondence authors; E-mails: viola.morris@emory.edu (V.B.M.); drsharmacp@yahoo.com (C.P.S.).

Abstract: The efficiency of gene transfection using cationic polymers primarily depends on factors such as compact polyplex formation, cellular uptake, endosomal escape, cytoplasmic transport, nuclear entry, and the dissociation and release of plasmid from the polyplex. These factors can be manipulated through the chemical modification of cationic polymers. Branched polyethyleneimine (PEI) has been considered the "gold standard" in gene delivery due to its superior transfection efficiency. However, cytotoxicity and serum sensitivity limit its therapeutic use. In the present study, we aimed to reduce cytotoxicity while maintaining or enhancing transfection efficiency by chemically modifying PEI with the amino acid histidine via five-armed alkylamino siloxane. We anticipated that the spatial orientation of histidine could enhance cellular uptake and endosomal escape. Histidine-modified PEI, termed P(S-His)1, improved gene transfection efficiency due to elevated cellular uptake through multiple pathways and rapid endosomal escape via the proton sponge effect, compared to PEI and other derivatives with higher histidine conjugation. When the same polymer was further chemically modified with polyethylene glycol-folic acid (PEG-FA) to facilitate receptor-mediated cellular targeting, cellular uptake improved through additional pathways; however, the transfection efficiency unexpectedly decreased. This reduction in transfection efficiency is likely due to the absence of plasmid release from the polyplex for gene transcription, caused by the reduced ionic strength of the polyplex resulting from the high molecular weight PEG.

Keywords: folate receptor; buffering capacity; endosomal escape; histidine; poly(ethyleneimine)

1. Introduction

Gene therapy using nonviral delivery systems is a promising approach due to its safety and reliability. Polyethyleneimine (PEI) is recognized as a highly efficient gene delivery vector because of its capacity to form stable complexes with various types of nucleic acids, such as plasmid DNA, siRNA and mRNA. However, the cytotoxicity and limited serum stability of PEI polyplexes impact their therapeutic use.

The heterocyclic imidazole group of histidine is a weak base having a pKa around 6, which allows it to absorb protons and possess buffering capacity. Several studies have reported that incorporating histidine into polymeric gene delivery vectors reduces cytotoxicity while improving gene transfection efficiency by increasing the endosomal buffering capacity of the polymer, thus enhancing the efficiency of endosomal escape [1–3]. It has also been observed that histidine-modified trimethylated chitosan with PEG-FA ligands shows enhanced cellular and nuclear uptake [4]. Kichler *et al.* reported that oligoalkylaminosiloxane synthesized via alkoxysilane condensation can deliver DNA into cells through adsorptive endocytosis via sulfated proteoglycans [5]. In our previous work, we found that the spatial orientation of arginine conjugated to PEI via oligoalkylaminosiloxane enhanced gene transfection efficiency in tumor cells, as well as in neurons and astrocytes, compared to the parent polymer PEI [6–9]. In the present study, we evaluated the effect of histidine on transfection efficiency and biocompatibility, replacing arginine. We anticipate that the heterocyclic imidazole group of histidine could enhance the buffering capacity of the cationic polymer, thereby improving transfection efficiency through rapid endosomal escape of the polyplex [10–12].

Receptor-mediated gene therapy enables the delivery of therapeutic genes to specific sites in the body to correct or supplement mutated genes responsible for diseases. This approach improves efficacy and reduces toxicity by altering the biodistribution of genes through specific interactions with cell surface receptors. Among various targeting groups or ligands used to target tumor cell-specific receptors, folic acid has been widely recognized as a targeting agent for various anti-cancer drugs [13,14]. The folate receptor, a glycosylphosphatidylinositol (GPI)-anchored protein, is known to be overexpressed in several tumors in human, including brain, lung, kidney, and breast cancers, particularly in epithelial carcinomas like ovarian cancers [15,16]. Consequently, folic acid has been conjugated covalently to anti-cancer drugs and gene delivery agents for selective targeting of tumors [17]. Rosenholm *et al.* reported that grafting folic acid (FA) conjugated PEI in mesoporous silica improved endosomal escape, reduced toxicity, and enhanced targetability [18].

In our present study, we aimed to achieve tumor cell specificity by modifying histidine-conjugated oligoalkylaminosiloxane-grafted PEI [P(S-His)1] with polyethylene glycol-folic acid (PEG-FA) [13]. As expected, histidine conjugation improved cell viability compared to the parent polymer, PEI, while maintaining transfection efficiency. However, the transfection efficiency of the PEG-FA conjugated P(S-His)1 polymer [P(S-His)1FP3] was lower than that of its parent polymer.

2. Materials and methods

2.1. Materials

3-(2-aminoethylamino) propyl-methyl-dimethoxysilane from fluka, folic acid, 25-kDa branched PEI, O-(2-aminoethyl)-O'- (2-carboxyethyl) polyethylene glycol-3000 hydrochloride and L-histidine were purchased from Aldrich, the luciferase protein expressing plasmid pGL3 control vector, Reporter Lysis Buffer and Luciferase 1000 Assay System were purchased from Promega. The Green fluorescent protein expressing plasmid, pEGFP-N3, (Clontech) was kindly provided by RGCB Thiruvananthapuram. Dicyclohexylcarbodiimide (DCC), 1-Ethyl-3-(3-dimethylaminopropyl) carbodiimide hydrochloride (EDC), N-hydroxysuccinimide (NHS), and 3-[4,5-dimethylthiazol-2-yl]-2,5-diphenyltetrazolium bromide (MTT), were purchased from Sigma (USA). Minimal Essential Medium (MEM), Fetal bovine serum (FBS) and Trypsin/EDTA were obtained from Gibco (USA). RPMI 1640 was obtained from Invitrogen.

2.2. Synthesis of histidine conjugated oligo (alkylaminosiloxane) (S-His)

Oligo- (alkylaminosiloxane) (SiDA) was prepared as reported elsewhere [5] . Briefly, basic hydrolysis of 1.8 mM, (1eq) of 3-(2-aminoethylamino) propyl-methyl- dimethoxysilane was performed using 1 equivalent of 1 N NaOH at room temperature for 20 h. The oligomers were exposed to reduced pressure to remove any volatiles. The crude sample was subsequently diluted to 5 mL with water and neutralized to pH 7 using 1 N HCl. The product was characterized by 1H1H NMR (Bruker Avance DPX 300) and mass spectrometry (Quattro Micro API mass spectrometer; m/z = 641, 143, 302, 321, 481, 802).

Histidine conjugated oligo- (alkylaminosiloxane) was prepared by EDC/NHS chemistry [8]. Briefly, the carboxylic acid group of L-histidine (5 eq) was activated using EDC/NHS at 4 ℃ for 4 hours in PBS at pH 8. SiDA (1 eq) was then added to the activated histidine, and the reaction was maintained for 18 hours at room temperature. The histidine-conjugated SiDA (S-His), was dialyzed (MWCO 1000) against deionized water to remove unreacted compounds and then lyophilized.

2.3. Synthesis of poly (ethyleneimine) grafted S-His [P(S-His)n]

S-His was coupled to PEI by EDC/NHS chemistry with N-BOC protected aspartic acid as the linker group [8]. In summary, the carboxylic acid group of aspartic acid was initially activated with half equivalents of EDC and NHS in PBS at pH 8 for 4 hours at 4 ℃. After activation, S-His (n eq), dissolved in PBS, was added to the mixture, and the reaction was allowed to proceed at room temperature for 18 hours. The reaction mixture was then dialyzed (MWCO 1000) to remove any unreacted reagents. Following this, the remaining carboxylic acid group on aspartic acid was reactivated with EDC and NHS at 4 ℃ for 6 hours. One equivalent of PEI was then introduced to the reaction mixture, which was left to react at room

temperature for an additional 18 hours. Finally, the resulting mixture was dialyzed (MWCO 12000) and lyophilized.

2.4. Synthesis of folic acid conjugated P(S-His)n [P(S-His)nFPn]

FA-PEG-COOH was synthesized according to the procedure reported elsewhere. [9,19].

2.5. Characterization of the polymers

FTIR spectra were recorded from 4000 to 650 cm^{-1} using a Shimadzu spectrophotometer. The molecular mass of the polymers was estimated using a Micromass Quattro Micro API mass spectrometer and gel permeation chromatography (GPC) (Waters Corporation, Washington, USA) at 25 ± 2 ℃. The GPC system consisted of an Ultra Hydrogel Linear column, a Waters 2410 refractive index detector, and a Waters 600E pump. The eluent was 0.5 M acetate buffer, and dextran standards (MW 10,000–200,000) were used to calibrate the column. The primary amine content of polymer solutions was determined by the TNBS assay at a concentration of 1 mg/mL in Milli-Q water. The thermal behavior of the polymers was evaluated by differential scanning calorimetry (DSC) using a Waters DSC with mass flow control. Briefly, 8–10 mg samples were encapsulated in aluminum pans and heated at a rate of 10 ℃/min from − 20 to 250 ℃. The conjugation of folic acid to the polymers was assessed by UV spectroscopy, using a molar extinction coefficient of 6197 mol^{-1} cm^{-1} at 363 nm.

2.6. Acid base titration

Acid base titration of the polymer was determined by protonation and positive charge generation [20]. Briefly, the polymer solution at 0.2 mg/ml in milli Q water was titrated to pH 10 with 0.1 N NaOH. The solution was later titrated with 0.1 N HCl in the pH range of 10^{-3}. The pH profile was obtained for PEI, P(S-His)n and its derivatives.

2.7. Preparation of polymer/pDNA (Polyplex) nanoparticles

The pGL3 and pEGFP plasmid DNAs, grown in *E. coli* (JM109) cells, were purified using a Qiagen QIAfilter Plasmid Mega Kit following the manufacturer's instructions and re-suspended in TE buffer. PEI, PEI-conjugated S-His derivatives at varying molar ratios [P(S-His)n], and their folate derivatives [P(S-His)nFPn] were dissolved in Milli-Q water at a concentration of 1 mg/mL. The filtered polymer solution (0.22 μm filter) was mixed with pDNA at a concentration of 2.5 μg/mL, prepared in 1 mg/mL in 5 mM PBS (pH 7.4). Keeping the pDNA weight constant, the polymer weight was adjusted to achieve polyplexes across a range of weight ratios, including 0.25, 0.5, 1, 3, 5, and 10. The solution was vortexed for 15 seconds and incubated at room temperature for 20 minutes to ensure complete complex formation.

2.8. Determination of particle size and zeta potential

Particle size and zeta potential of the polyplex nanoparticles after 20 min of preparation were estimated using Zetasizer Nano ZS (Malvern Instruments Ltd., UK).

2.9. Gel retardation assay

Polyplex formation was further analyzed by agarose gel electrophoresis. Polyplex nanoparticles, prepared at w/w ratios of 0.25, 0.5, 1, 3, 5, and 10, along with the naked plasmid, were loaded onto a 1% agarose gel in Tris-Acetate-EDTA (TAE) buffer at pH 8.0. Electrophoresis was performed at 100 V for 30 minutes. The gel was then stained with ethidium bromide and imaged using a phosphor-imager (FUJIFILM FLA-5100).

2.10. Fluorescamine assay

Fluorescamine assay was used to estimate the degree of polyplex formation by quantifying the free amino groups before and after complexation with DNA [21]. Briefly, 10 µL of the nanoparticle solution was diluted to 150 µL with 100 mM boric acid-NaOH buffer (pH 8) in a 96-well plate. Wells containing only the boric acid assay buffer served as blanks. To each well, 50 µL of 0.01% fluorescamine solution in acetone was added, mixed thoroughly, and incubated for 10 minutes at room temperature. Fluorescence was measured at an excitation wavelength of 390 nm and an emission wavelength of 475 nm using a TECAN Infinite M200 (monochromator-based) multi-mode plate reader (Austria).

2.11. DNase I protection assay

Protection of pDNA within polyplex by the polymer was evaluated by checking any variation in the absorbance of polyplex solutions at 260 nm after applying DNase1 with the polyplex [22]. Polyplex solutions were prepared at the desired w/w ratios with a final DNA concentration of 20 µg/mL (corresponding to an absorbance of 0.4 at 260 nm) in TE buffer (pH 7.5). After incubating the polyplexes for 20 minutes, DNase I was added at a concentration of 100 IU (5 IU/µg DNA) along with 10× DNase I buffer, bringing the final volume of the polyplex solution to 1 mL. The change in absorbance at 260 nm was then monitored. PEI served as the positive control, while naked DNA served as the negative control.

2.12. Evaluation of morphology of the polyplex nanoparticles by AFM and TEM

The morphology and size distribution of polymer/pDNA nanoparticles were analyzed by transmission electron microscopy (TEM) using a Hitachi H7650 instrument at 100 kV, and by atomic force microscopy (AFM) (WITEC Confocal Raman Microscope System with an AFM extension Germany). The polyplexes were prepared by mixing 1 µg of plasmid DNA with an aqueous polymer solution at optimal weight ratios to achieve a final DNA concentration of 10 ng/µL. After 20 minutes of incubation, 10 µL of the nanoparticle suspension was used for TEM and AFM analysis. For TEM, a drop of the sample was placed

on a copper grid, excess liquid was removed with filter paper, and the grid was air-dried. For AFM, the nanoparticles were placed on a freshly cleaved untreated mica surface and allowed to adhere for 1–2 minutes. Excess solution was carefully removed by absorbing it with filter paper, and the mica surface was further dried at room temperature for 24 hours. The imaging was performed in tapping mode with a scanning speed of 1–5 Hz.

2.13. Cell culture

Human nasopharyngeal epidermoid carcinoma cells (KB cells) were cultured in MEM supplemented with 10% FBS and 1% penicillin-streptomycin, and maintained under conditions of 5% CO_2 and 95% humidity at 37 ℃.

2.14. Evaluation of cytotoxicity

The cytotoxicity of the polymers and polyplexes with pDNA was evaluated using the MTT assay. KB cells were seeded in a 96-well tissue culture plate at a density of 5×10^3 cells/well in 100 µL of MEM containing 10% FBS. Once the cells reached 70–80% confluence after 24 hours, they were exposed to 10 µL of polymers at various concentrations (25, 50, 75, and 100 µg/mL) in 90 µL of MEM with 10% FBS. After 24 hours, the medium containing the polymers was removed, and 26 µL of MTT (2 mg/mL in MEM) was added. The cells were incubated for 4 hours under normal growth conditions. After incubation, the MTT solution was replaced with 150 µL of DMSO. Absorbance was measured at 620 nm after 30 minutes of incubation at 37 ℃ using a plate reader. Cells without polymer treatment were used as the control.

To evaluate the cytotoxicity of polyplex nanoparticles, 1×10^5 cells/well were seeded in a 24-well plate with 100 µL of MEM containing 10% FBS. After 24 hours, polyplexes of each polymer at its optimal weight ratio, containing 2.5 µg of DNA, were added to the cells. After 24 hours of polyplex incubation, the cells were washed twice with PBS, and 200 µL of MTT at a concentration of 0.5 mg/mL in MEM was added. The cells were incubated at 37 ℃ under 5% CO_2 for 4 hours. After incubation, the MTT solution was removed, and 200 µL of DMSO was added to each well. Absorbance was measured at 620 nm.

Cell Viability = $[Abs]_{sample} / [Abs]_{Control} \times 100$.

2.15. In vitro transfection studies

KB cells were seeded at a density of 1×10^5cells/well in a 24-well plate. The medium was replaced with RPMI 1640 supplemented with 10% FBS and 1% penicillin–streptomycin. The cells were treated with a polyplex solution in 250 µL of RPMI 10% FBS, containing 2.5 µg of plasmid DNA at an optimal weight ratio of 1:2, for 3.5 hours at 37 ℃. After exchanging with fresh medium, the cells were further incubated for 48 hours at 37 ℃. The cells were then washed twice with DPBS and lysed in 100 µL of Reporter Lysis Buffer (Promega). Luciferase activity was measured by transferring 25 µL of the lysate into a white 96-well plate and adding 50 µL of Luciferase Assay Reagent (Promega). The reading was taken using

a Hidex Chameleon Plate Reader with a 10-second integration time and a 2-second measurement delay. A protein assay was performed using the Micro BCA Protein Assay Reagent Kit (Pierce). Results were reported as RLU/mg cellular protein. Branched PEI with a molecular weight of 25 kDa was used as a positive control.

The transfection efficiency of folate-conjugated and non-conjugated polymers was evaluated using a green fluorescent protein-expressing plasmid DNA (pEGFP). KB cells were seeded at a density of 1×10^5 cells/well in a 4-well plate with medium containing 10% FBS. The cells were treated with polyplexes of P(S-His)1FP3, P(S-His)1, and PEI, each containing 2.5 µg of plasmid DNA (pEGFP) at the optimal weight ratio of 1:2 for 3.5 hours at 37 ℃. After exchanging the medium, the cells were further incubated for 48 hours, and the fluorescence of the expressed GFP was visualized using a confocal laser scanning microscope with an Argon/2 laser.

2.16. In-Vitro targeting of the polymers

The uptake of folate-conjugated and non-conjugated P(S-His)1 were evaluated by flow cytometry using fluorescein isothiocyanate (FITC) tagged polymers. FITC was tagged to the primary amino groups of the polymers by mixing 1 mg/ml of the polymer with 100 µl of 0.5 mg/ml FITC in bicarbonate buffer at pH 9 for 2h at room temperature in dark. The reaction was stopped by adding 100 µl of hydroxylamine hydrochloride (1.5M) solution at pH 8.5. The FITC tagged polymers were then dialyzed in water overnight to remove unreacted reagents.

Adherent KB cells were cultured in 24-well plates in RPMI medium (folic acid-free) supplemented with 10% FBS and 1% penicillin-streptomycin (Sigma-Aldrich). FITC-tagged nanoparticle derivatives were added to the cells when they reached 80% confluence and incubated for 4 hours at 37 ℃. After incubation, the cells were washed once with PBS and treated with 0.4% trypan blue solution to quench extracellular fluorescence. The cells were then washed three times with PBS and fixed in 1% paraformaldehyde solution for 30 minutes at 4 ℃. After fixation, the cells were washed twice with PBS. The cell suspensions were analyzed using a BD FACS Aria cell sorter (BD Biosciences), with 10,000 cells evaluated per experiment. Data acquisition and analysis were performed using BD FACSDiva software (BD Biosciences).

2.17. Nuclear localization of P(S-His)1FP3/DNA nanoparticles

P(S-His)1FP3 polymer was tagged with FITC and polyplex was formulated with plasmid DNA. The polyplex with 1 µg of plasmid at optimal weight ratio of 1:2 were incubated with KB cell lines for 4 hours in a 4 well plate and nuclear staining was done with Hoechst 33342. Post incubation of 4, 24 and 48 hours, the cells were then viewed under Leica Fluorescence microscope (Leica DMI 3000 B Trinocular Inverted Research Microscope, Germany).

2.18. Treatment with inhibitors

KB cells were seeded at a density of 1 $X10^5$ cells/well in a 24-well plate. After 24 hours of incubation in normal conditions, cells were pre-treated with genistein (200 µM), wortmannin (100 nM), or chlorpromazine (10 µg/mL) [23] and 1 mM folic acid for 1 hour before addition of polyplexes. Polyplex of P(S-His)1FP3, P(S-His)1 and PEI containing 2.5 µg of plasmid DNA (pEGFP) at its optimum weight ratio of 1:2 were treated with cells for 3.5 hours at 37 ℃. Then the cells were washed with PBS and supplemented with fresh media containing 10% serum and further incubated for 2 days before assay.

3. Results and discussion

3.1. Synthesis and characterization of P(S-His)n and P(S-His)1FPn derivatives

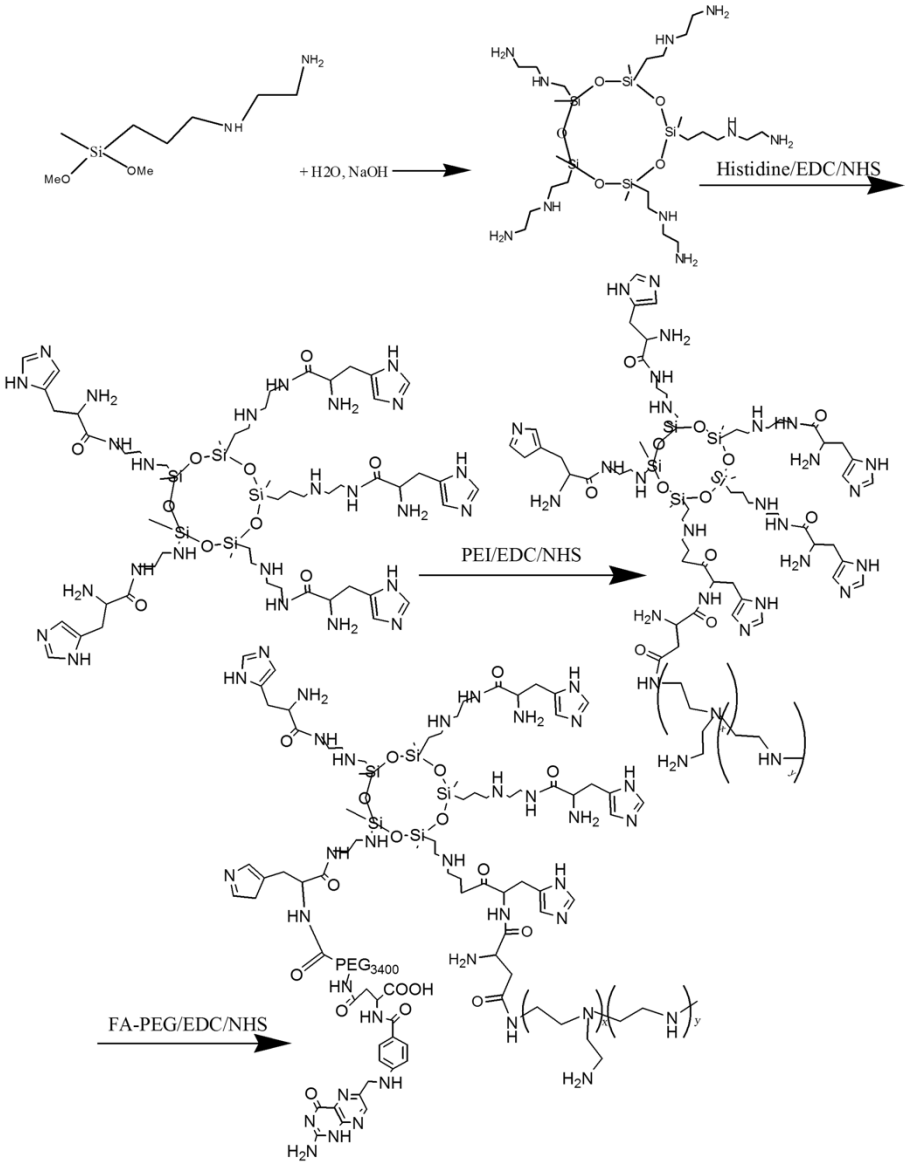

Scheme 1. Reaction scheme of P(S-His)nFPn derivative**.**

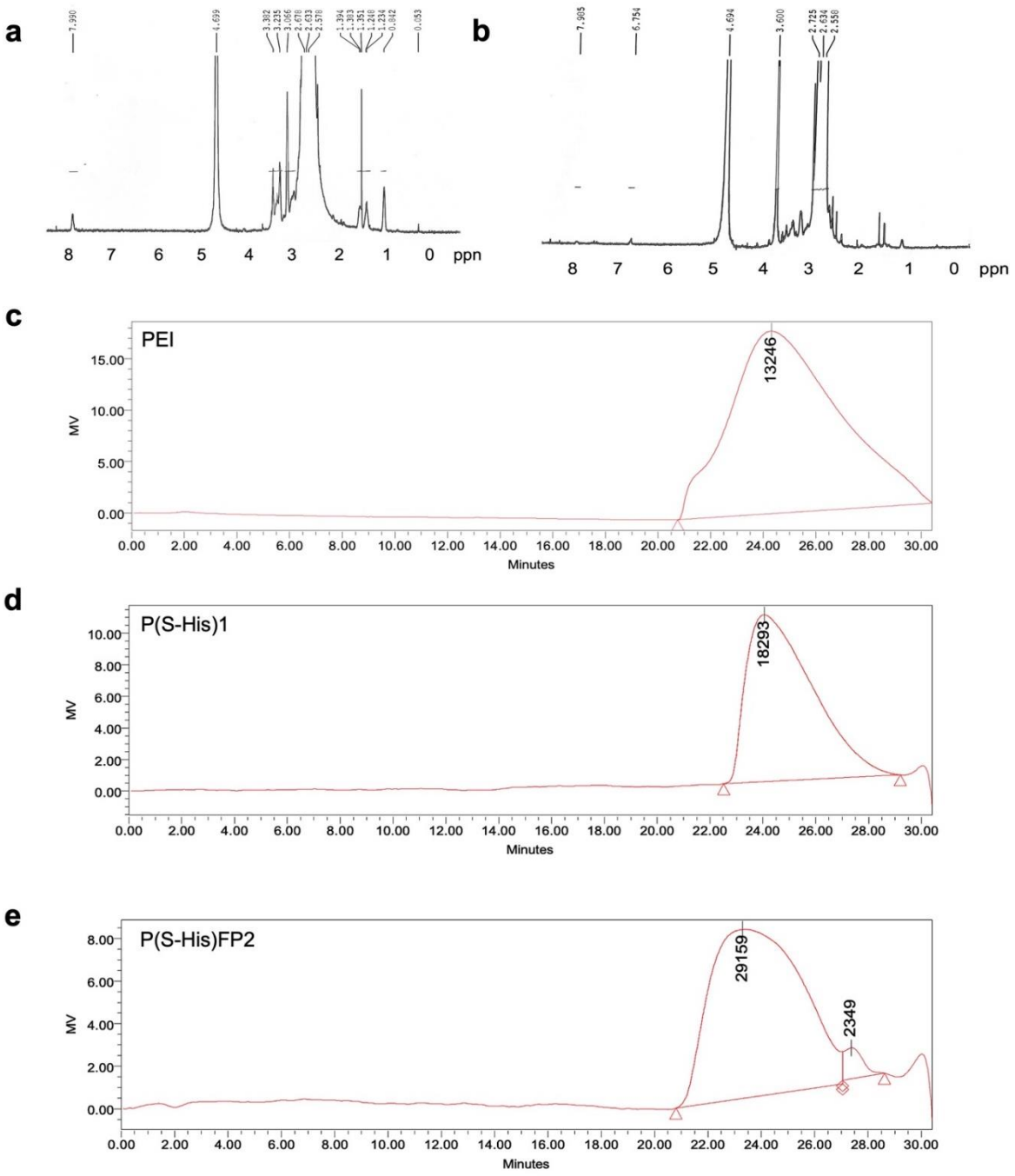

Figure 1. Chemical characterisation of polymer derivatives**. a, b,** ^{1}H NMR spectra of P(S-His)1 (a) and, P(S-His)1FP2 (b) derivatives. **c–e,** Gel permeation chromatography curves of PEI (c), P(S-His)1(d) and P(S-His)1FP2 (c).

To improve the endosomal buffering capacity of PEI and thus to enhance transfection efficiency without compromising cell viability, histidine was conjugated to PEI using oligo(alkylaminosiloxane) as a flexible spacer (Scheme 1). By keeping the composition of PEI constant, the molar equivalents of histidine-conjugated oligo(alkylaminosiloxane) (S-His) were varied to obtain P(S-His)1, P(S-His)5, P(S-His)10, and P(S-His)15. The conjugation of S-His to PEI was confirmed by IR and NMR spectroscopic analyses. The prominent IR peak at 1637 cm^{-1} indicated the formation of an amide bond (Figure S1). NMR

peaks at 7.2 and 8.2 ppm indicated the presence of the heteroaromatic compound histidine (Figure 1a). Additionally, the increased molecular weight of P(S-His)1 compared to PEI was evidenced by the GPC curve, which showed a peak shift from 13246 to 18293, further confirming the successful formation of histidine conjugates (Figure 1c, d).

To achieve tumor cell specificity, P(S-His)1 was subsequently conjugated with PEG-FA in two compositions, designated as P(S-His)1-FP2 and P(S-His)1-FP3. These designations indicate the molar equivalents of PEG-FA with respect to P(S-His)1. The conjugation of PEG-FA to P(S-His)1 resulted in a shift of the IR peak for –CO-NH- from 1629 cm^{-1} to 1647 cm^{-1}. Additionally, new amine peaks of PEG-FA were observed at 1307 cm^{-1} in the derivatives P(S-His)1-FP2 and P(S-His)1-FP3, confirming the successful conjugation with PEG-FA (Figure S2). A sharp NMR peak at 3.6 ppm also confirmed the presence of PEG (-CH2CH2O-) in P(S-His)1-FP. The methylene peaks of PEI and PEG groups were observed at 3.36–3.38 ppm and at 3.6 ppm, respectively. Furthermore, the presence of aromatic proton signals at 6.75 ppm confirmed the conjugation of folic acid (Figure 1b). The GPC curve further validated the conjugation of folic acid to P(S-His)1, showing an increase in molecular weight from 18293 to 29159 for P(S-His)1-FP2 (Figure 1e).

Differential scanning calorimetric (DSC) analysis (Table 1) was used to further evaluate the formation of S-His and PEG-FA conjugates with PEI. The increase in their thermal properties, specifically the glass transition temperature (Tg) and melting temperature (Tm) with increasing concentrations of S-His confirmed its chemical conjugation to PEI. Similarly, when PEG-FA was conjugated to P(S-His)1, its Tg and Tm values increased from 102 ℃ to 131 ℃ and from 122 ℃ to 142 ℃, respectively, for P(S-His)1FP2. As the concentration of PEG-FA increased further, the Tg and Tm values increased to 142 ℃ and 155 ℃, respectively, for P(S-His)1FP3. The increase in these values suggests successful chemical conjugation, as well as enhanced molecular interactions and structural stability in the modified materials.

Table 1. DSC data of the P(S-His)n derivatives before and after PEG-FA conjugation.

Polymer	Tg	Tm
PEI		96.74
P(S-His)1	102.93	122
P(S-His)5	113	130
P(S-His)10	132.36	167.23
P(S-His)15	141.68	170.54
P(S-His)1FP2	131.97	152.83
P(S-His)1FP3	142.84	155.94

The free amino groups of the P(S-His) derivatives were estimated using the TNBS assay (Figure 2a). At lower concentrations of S-His residues, there was no significant difference in

the amount of primary amino groups compared to PEI. However, as the concentration of S-His residues increased from 5 to 15 equivalents, the degree of primary amino groups decreased. This reduction might be due to the replacement of primary amino groups with the imidazole groups of histidine, which were involved in amide formation with the acid groups of histidine.

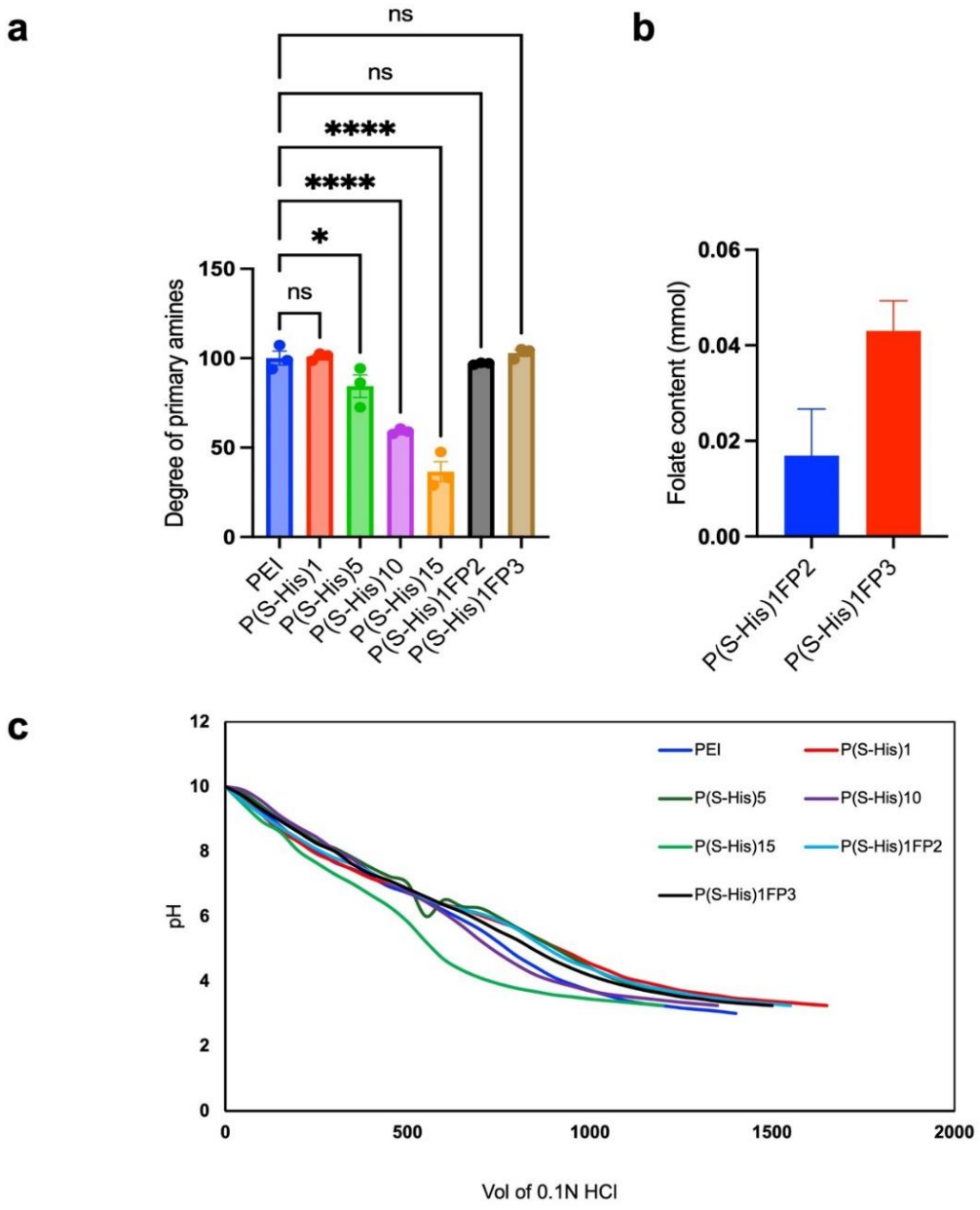

Figure 2. Characterization of polymers. **a,** Primary amine content of P(S-His)n and folate derivatives using TNBS assay. **b,** Folic acid content of the P(S-His)1FPn derivatives determined by UV spectroscopy analysis of FA using a molar extinction coefficient of 6197 $mol^{-1}cm^{-1}$ at 363 nm. Data of 'b' and 'c' presented as mean ± S.E.M.; three independent experiments, each with technical replicates. **c,** Acid /base titration of P(S-His)n and folate derivatives. PEI is considered as positive control.

This further confirmed the conjugation of S-His to PEI. There was no significant change in the degree of primary amino groups after the conjugation of PEG-FA to P(S-His)1, likely because the primary amino groups of P(S-His)1 were replaced by the primary amino groups of FA. As the level of PEG-FA conjugation increased, the amount of primary amino groups also increased. The increase in folic acid conjugation was further confirmed through UV spectroscopy analysis of FA, using a molar extinction coefficient of 6197 mol^{-1} cm^{-1} at 363 nm, which revealed values of 0.017 mmol g^{-1} and 0.043 mmol g^{-1} for P(S-His)1FA2 and P(S-His)1FA3, respectively (Figure 2b).

The acid-base titration data of the P(S-His) derivatives demonstrated the buffering capacity of the polymers, which correlates with their ability to disrupt endosomes after cellular uptake (Figure 2c). Due to the high pKa value of the imidazole group in the histidine residue, P(S-His)1 and P(S-His)5 derivatives exhibited a higher buffering capacity than PEI. However, as the concentration of S-His increased further, the buffering capacity decreased. This suggests that both the imidazole group and the primary amino groups play a significant role in the buffering capacity of the cationic polymers. The conjugation of PEG-FA to P(S-His)1 did not result in any significant change in buffering capacity.

3.*2. Formulation of polyplex nanoparticles and their characterization*

Polyplex nanoparticles of PEI and its derivatives, P(S-His)n and P(S-His)1FPn, were prepared with plasmid DNA (pGL3 Luciferase reporter vector) at varying polymer concentrations while keeping the pDNA constant, to optimize the appropriate weight ratio. Dynamic light scattering (DLS) was performed to evaluate nanoparticle formation (Figure 3a,b). Among the various weight ratios tested—0.5, 1, 2, 3, 4, and 5—an N/P (w/w) ratio of 2 was considered optimal, as it provided the smallest particle size and the most suitable cationic charge for all the derivatives. Interestingly, the overall surface charge of the PEG-FA-conjugated derivatives was reduced by half compared to the parent polymer P(S-His)1, despite no significant difference in the primary amino groups among the polymers.

Polyplex formation was further confirmed using a gel retardation assay via agarose gel electrophoresis. By keeping the DNA weight constant and varying the weight of the polymers in ratios of 0.25, 0.5, 1, 2, 3, 4, and 5, the ability of the polymers to retard DNA was evaluated. For lower S-His conjugation to PEI, such as P(S-His)1 and P(S-His)5, DNA was completely retarded within the wells of the agarose gel from an N/P (w/w) ratio of 0.25 onwards. However, for higher conjugations like P(S-His)10 and P(S-His)15, DNA was fully retarded within the wells only from an N/P (w/w) ratio of 0.5 onwards. This indicates that the presence of primary amino groups is essential for polyplex formation (Figure 3c).

In the case of PEG-FA conjugated derivatives of P(S-His)1, the derivative P(S-His)1FP2 retarded DNA from an N/P (w/w) ratio of 0.25 onwards, compared to P(S-His)1FP3. This suggests that although the primary amino groups of PEI were replaced by those from FA, they might not have been involved in complex formation because they were positioned away from the cationic core by the long PEG spacer chain (Figure 3d).

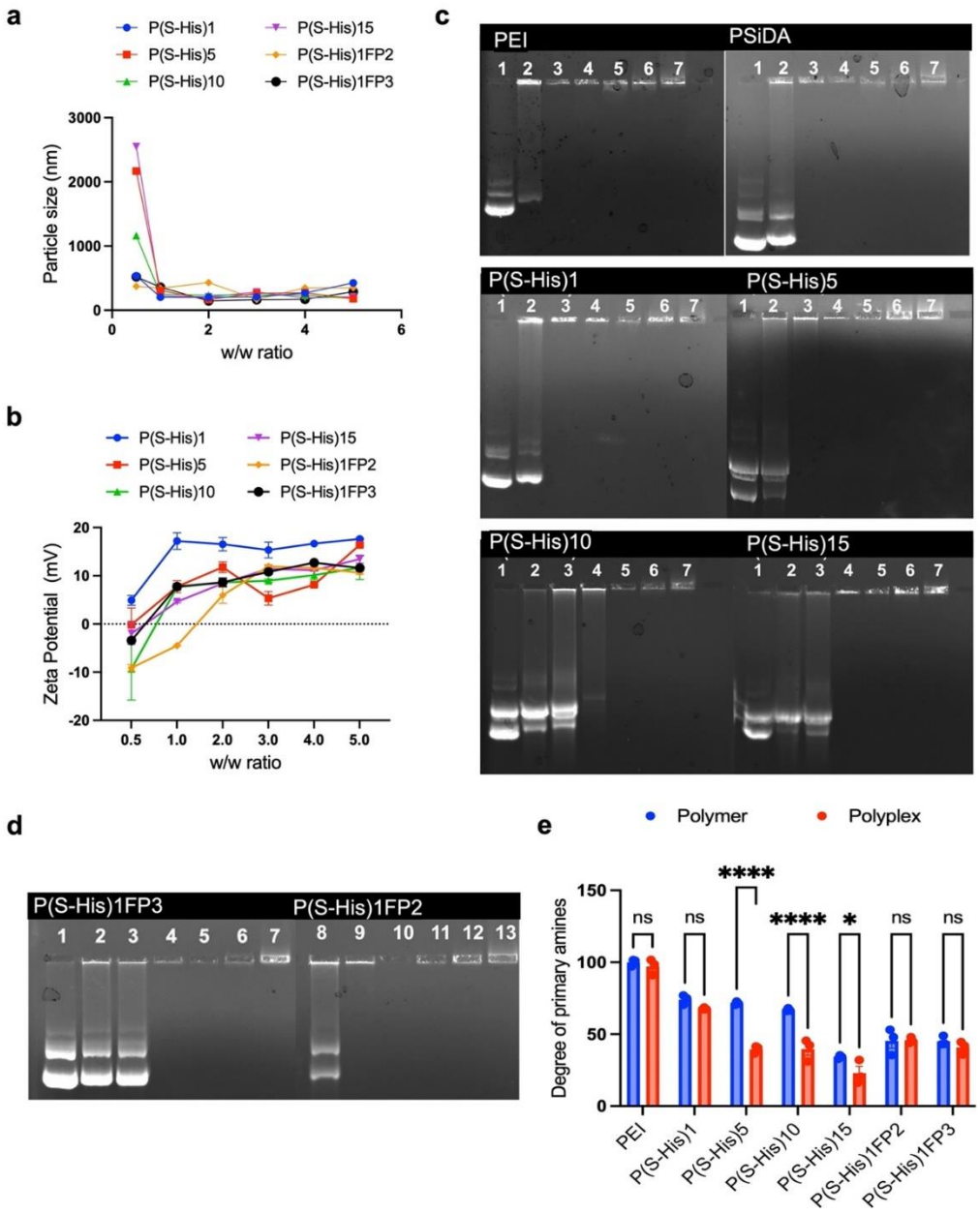

Figure 3. Electrostatic complex formation of plasmid DNA (pGL3 Luciferase reporter vector) by polymer (polyplex) and its properties**. a, b,** Particle size and zeta potential of polyplex nanoparticles formulated by P(S-His)n and its PEG-FA derivatives. **c**, Agarose gel electrophoresis representing polyplex formation of pDNA by P(S-His)n at different w/w ratios. Lane1: pDNA alone, Lanes 2–7 are Polymer/pDNA at w/w ratios of 0.25, 0.5, 1, 3, 5 and 10. **d**, Agarose gel electrophoresis representing polyplex formation of pDNA by P(S-His)FP3 and P(S-His)FP2 derivatives at different w/w ratios. Lane1: pDNA alone, Lanes 2–7 are P(S-His)FP3 /pDNA at w/w ratios of 0.25, 0.5,1, 3, 5 and 10 and lanes 8–13 are P(S-His)FP2 /pDNA at w/w ratios of 0.25, 0.5,1, 3, 5 and 10. **e,** Estimation of free amino groups on P(S-His)n and its folate derivatives before and after electrostatic complex formation with pDNA by fluorescamine assay. Data presented as mean ± S.E.M.; three independent experiments, each with technical replicates.

The fluorescamine assay was also used to verify polyplex formation by estimating the primary amino groups before and after complexation with DNA (Figure 3e). For polymers with a high concentration of primary amines like PEI, such as P(S-His)1, P(S-His)1FP2, and P(S-His)1FP3, based on the TNBS assay (Figure 2a), there was no significant difference in the number of amino groups before and after complexation with DNA. However, for polymers like P(S-His)5, P(S-His)10, and P(S-His)15, which had significantly fewer primary amino groups compared to PEI, a significant difference in primary amino groups was observed before and after polyplex formation. This data validated the surface charge of the polyplex nanoparticles (Figure 3b), indicating that the excess primary amino groups present in P(S-His)1 after polyplex formation might enhance cellular uptake due to electrostatic interactions with the net negative charge of the plasma membrane [24,25].

The size and morphology of the polyplex nanoparticles were assessed using atomic force microscopy (AFM) and transmission electron microscopy (TEM). Both AFM and TEM images revealed spherical nanoparticles with uniform distribution (Figure 4a-c).

The stability of the polyplex against nuclease degradation is essential for maintaining the integrity of DNA after cellular uptake [26]. The nuclease resistance was evaluated by measuring the change in absorbance of the polymer/pDNA complex solution at 260 nm upon the addition of DNase I at a concentration of 5 IU/µg of DNA. The polyplexes of the folate derivative, P(S-His)1FP3, were tested as a representative polymer, while polyplexes of PEI/DNA and naked DNA complexes served as positive and negative controls, respectively. In the case of naked DNA, an immediate increase in the absorbance of the solution was observed due to the fragmentation of pDNA (Figure 4d). No degradation was observed with the polyplex nanoparticles. Both PEI and P(S-His)1FP3 provided similar protection for DNA against nuclease degradation.

***3.**3. Effect of histidine and folate derivatives on cell proliferation*

The effects of histidine and folate derivatives on cell proliferation were investigated to assess their potential as therapeutic agents. The cell viability of the polymer derivatives and their polyplex nanoparticles was evaluated using the MTT assay. Polymers were tested at four concentrations: 25 µg/ml, 50 µg/ml, 75 µg/ml, and 100 µg/ml in KB cell lines for 24 hours. At the lower concentration of 25 µg/ml, all derivatives were non-toxic compared to the parent polymer PEI at the same concentration (Figure 5a). Starting from a concentration of 50 µg/ml, the polymers began to exhibit toxicity to the cells. Interestingly, since the maximum polymer required for complete complex formation is only 2 µg per µg of plasmid DNA, all histidine derivatives of PEI can be considered non-toxic within the working range.

To test the toxicity induced by polyplex nanoparticles, 2.5 µg of plasmid DNA was used with polymers at their optimal weight ratios (w/w = 1:2). Despite the excess cationic charge after complexation, P(S-His)1/DNA exhibited the least toxicity to KB cell lines (Figure 5b). However, increasing the concentration of S-His conjugation to PEI augmented its toxicity to the cells, potentially due to the overcrowding of siloxane and histidine conjugates [5]. Polyplexes of polymers modified with PEG-FA further improved cell viability compared to

the control (Figure 5b). This enhancement may be attributed to the presence of folic acid, which could act as a supplement for cellular metabolic activities and the proliferation of KB cells [27,28]. Additionally, the PEG polymers are expected to reduce the overall surface charge, thereby decreasing non-specific interactions between the polymers and cellular components [23]. This reduction contributes to the improved cell viability observed in P(S-His)1FP2 and P(S-His)1FP3.

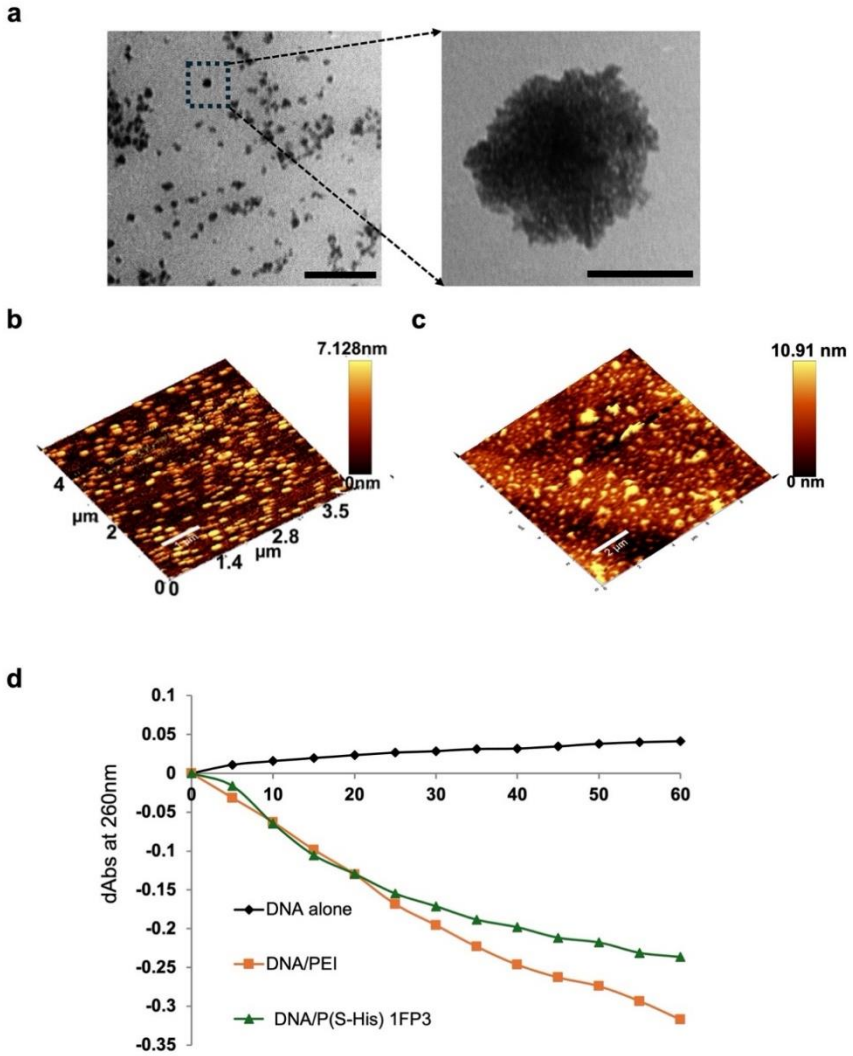

Figure 4. Morphological evaluation of polyplex formation and its stability against nuclease degradation. **a,** TEM micrograph of polyplex formulated by P(S-His)1 at optimum ratio. Scale bar: 200 nm and 100 nm for magnified image. **b, c,** 3D AFM images in the tapping mode of the P(S-His)1/pDNA and P(S-His)1FP3/pDNA complex respectively. d, Resistance of P(S-His)1FP3/pDNA complex against DNase I activity at w/w ratio of 2. DNase of 5 IU / µg of DNA were used. PEI/DNA complex was used as positive control at its optimum ratio. The DNA used was pGL3 Luciferase reporter vector.

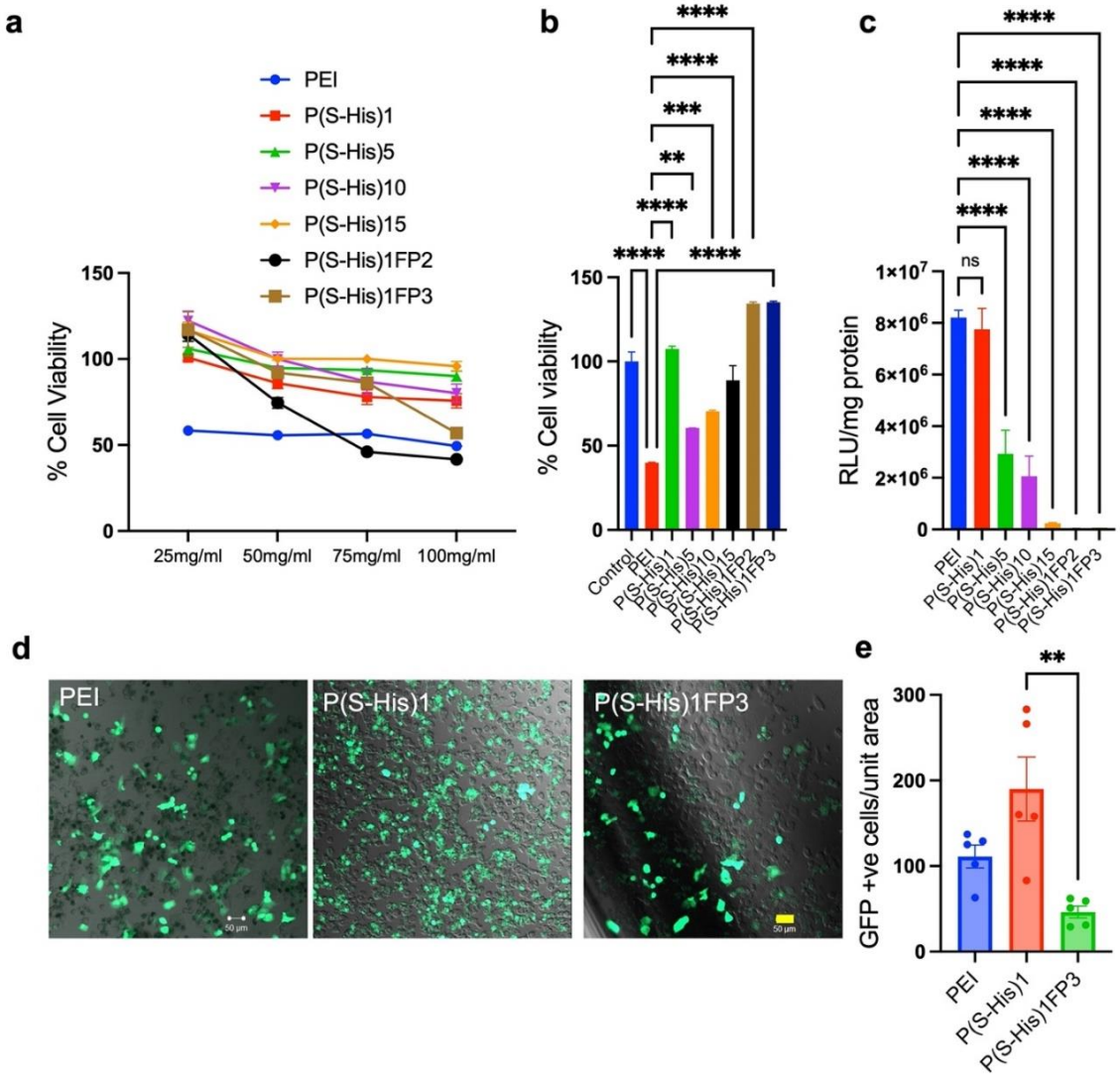

Figure 5. Cell viability and transfection efficiency of histidine and folate derivatives. **a,** The effect of P(S-His)n and folate derivatives on cell viability and proliferation of KB cell lines at varying concentration. PEI was used as control. **b,** The effect of polyplex formulated by P(S-His)n and folate derivatives at their optimum weight ratios on cell viability and proliferation of KB cell lines. PEI was used as control. **c,** In-vitro transfection efficiency in terms of relative luminescence units /mg protein expressed by polyplex formulated by P(S-His)n and folate derivatives in KB cell lines. Data presented from a-c as mean ± S.E.M.; three independent experiments, each with technical replicates. **d, e,** Confocal micrographs showing GFP expressed in KB cell line transfected of polyplex formulated by PEI, P(S-His)1 and P(S-His)1FP3 at their optimum weight ratios with complexes at their optimum ratios and its quantification expressed in number of GFP positive cells per unit area. Scale bar: 50 µm.

3.4. Effect of histidine and folate derivatives on gene transfection efficiency

The effects of histidine and folate derivatives on gene transfection efficiency were assessed to evaluate their potential as delivery vectors for plasmid DNA. The transfection efficiency

of these histidine and folic acid-conjugated derivatives was evaluated in KB cell lines using pGL3 and pEGFP control vectors. PEI was used as a positive control under optimal conditions. All experiments were conducted in the presence of 10% fetal bovine serum (FBS). Figure 5c illustrates the luminescence of the protein expressed by the pGL3 polyplex formulated with histidine and folic acid-conjugated derivatives in KB cell lines.

The polyplex of P(S-His)1 demonstrated comparable protein expression to that of PEI, despite being the least toxic to the cells. However, increasing the histidine conjugation resulted in a decrease in transfection efficiency. This observation aligns with the TNBS assay and DLS analysis, which indicated a reduced degree of primary amino groups and surface charge as histidine conjugation increased. The overcrowding of histidine groups may have concealed the remaining primary amino groups of the parent polymer, PEI. This suggests that although the imidazole group of histidine can enhance the proton sponge effect, an excess cationic surface charge from primary amino groups is indispensable for complete polyplex formation and effective cellular uptake. Similarly, while PEG-FA was expected to promote receptor-mediated cellular uptake, both luminescence and green-fluorescent expression of polyplexes formulated using the P(S-His)1FP3 derivative were further reduced (Figure 5d). Although both P(S-His)1FP2 and P(S-His)1FP3 derivatives exhibited comparable degrees of primary amino groups and low toxicity, the decreased transfection efficiency may be attributed to the reduced surface charge of the polyplex (Figure 3b).

3.5. Effect of histidine and folate derivatives on cellular and nuclear uptake

To further investigate the reasons for the reduced transfection efficiency of the PEG-FA conjugated P(S-His)1 derivative, the efficiency of cellular uptake of the polyplex nanoparticles in KB cell lines was evaluated. Flow cytometry evaluations revealed that PEG-FA conjugation enhanced cellular uptake of the polyplex nanoparticles compared to those formulated with the parent polymer P(S-His)1 by approximately 8% (Figure 6a–c). Moreover, fluorescent microscopic images showed that polyplexes formulated with FITC-stained P(S-His)1FP3 underwent cellular and nuclear uptake starting from 4 hours post-transfection (Figure 6d). However, the polymer began to clear from the cytoplasm after 24 hours, although it remained in the nucleus. The prolonged presence of polymers in the nucleus suggests that the polyplex might not be dissociating and releasing the plasmid for gene transcription. The PEG group in the P(S-His)1FP3 derivative may have hindered polyplex dissociation by reducing ionic strength due to the steric effects of high molecular weight PEG. Overall, these data indicate that while targeted derivatives of the polymer enhance cellular and nuclear uptake, transfection efficiency was depending on other cellular events, such as polyplex dissociation and plasmid release [29–32]. Furthermore, the bulkiness of the PEG group used to connect P(S-His)1 and folic acid may have impaired the efficient transportation of the polyplex through the cytosol.

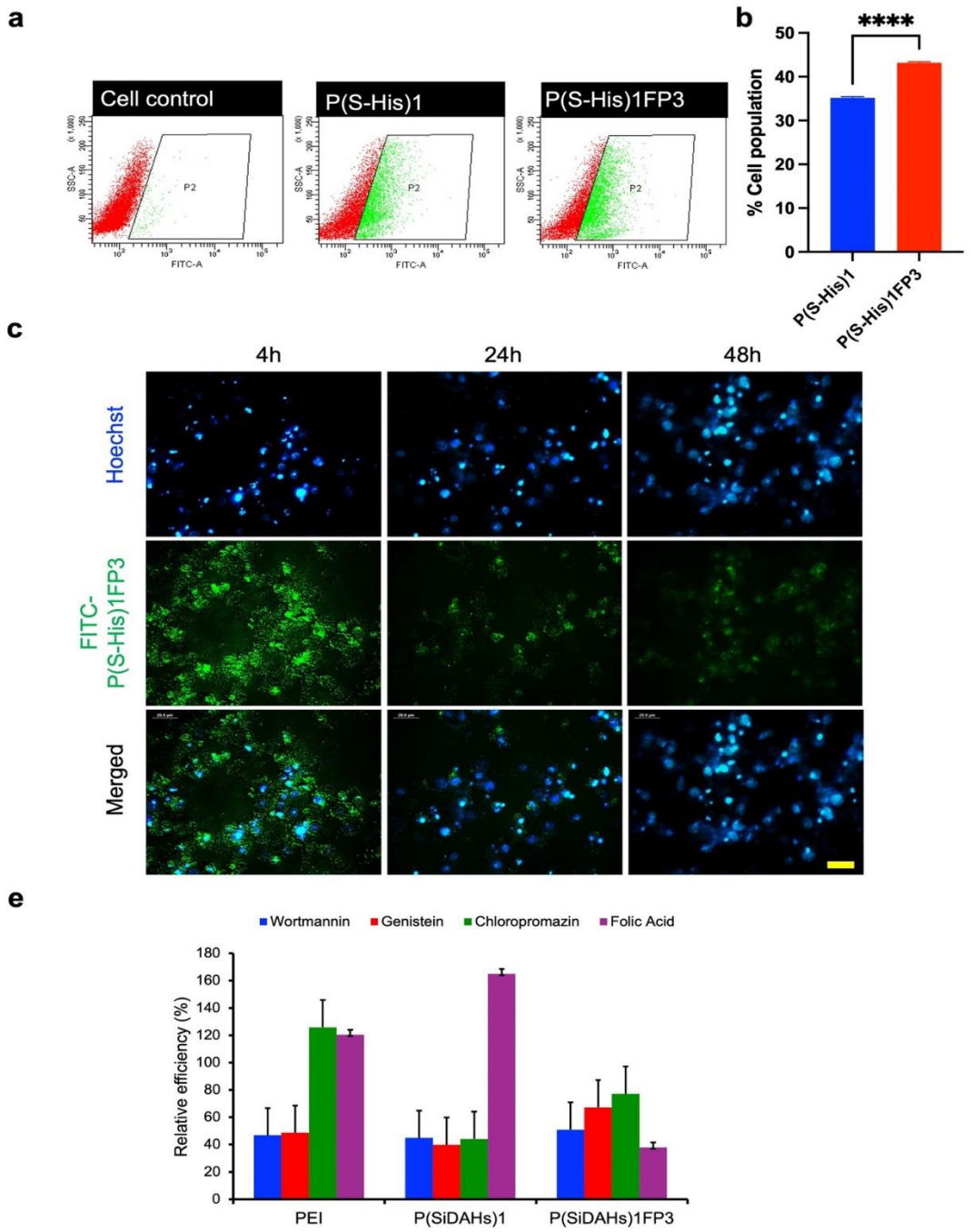

Figure 6. Cellular uptake of polyplex nanoparticles. **a, b,** In vitro folate receptor mediated cellular uptake of FITC stained P(S-His)1 and its folate derivative P(S-His)1FP3 in KB cell lines at 4 h post incubation estimated by flow cytometry. Cells without any staining was used as gating control. **c,** Fluorescent microscopic images of cellular and nuclear uptake of polyplexes formulated by FITC stained P(S-His)1FP3 at 4h, 24h and 48h after addition of polyplex into KB cell lines Scale bar: 20 μm. e, Relative transfection efficiency (RTE) of P(S-His)1FP3/pDNA complexes in presence of various endocytosis inhibitors. Polyplexes of P(S-His)1 and PEI were used as control polymers. The polymers without inhibitors (W.O.inhibitors) are considered as 100% . RTE= experimental value/control value × 100 (%). Data of c and e presented as mean ± S.E.M.; three independent experiments, each with technical replicates.

3.6. Effect of histidine and FA on cellular uptake pathways

Previous studies have reported that the enhanced transfection efficiency of arginine-conjugated polymers is due to their cellular uptake through multiple pathways [7,33]. To examine the effect of histidine and FA on cellular uptake pathways, the transfection efficiencies of P(S-His)1 and its PEG-FA conjugated derivative were assessed in the presence of various cellular uptake inhibitors, namely, wortmannin, genistein, chlorpromazine, and folic acid, with PEI serving as a control polymer. Genistein inhibits caveolae-mediated uptake processes [34] while wortmannin inhibits phosphatidylinositol-3-phosphate (PI3) kinase, thereby disrupting macropinocytosis. Chlorpromazine blocks clathrin-mediated endocytosis, and folic acid is projected to inhibit folate receptor-mediated endocytosis [18,35,36]. From Figure 6e, it is observed that, in contrast to PEI, for which transfection efficiency was influenced only by inhibitors of micropinocytosis and caveolae-mediated cellular uptake, the transfection efficiency of both P(S-His)1 and P(S-His)1FP3 was also influenced by clathrin-mediated endocytosis. This suggests that histidine conjugation enabled an additional pathway for cellular uptake alongside micropinocytosis and caveolae-mediated processes. Furthermore, the transfection efficiency of P(S-His)1FP3 was significantly affected by folate receptor-mediated endocytosis compared to all other cellular uptake pathways.

Interestingly, the transfection efficiency of P(S-His)1 increased to 160% when treated with folic acid. This enhancement may be attributed to either the increased metabolic activity and proliferation of the cells induced by folic acid or the formation of molecular aggregates between folic acid and the polyplex. Such hydrophobic particles could interact more efficiently with the cell membrane, leading to enhanced transfection [27,28,37].

4. Conclusion

The aforementioned studies using histidine and folic acid conjugated derivatives revealed that the transfection efficiency of polyplex nanoparticles depends not only on the overall positive charge and biocompatibility but is also significantly influenced by cellular uptake pathways, endosomal escape, efficient transportation through the cytosol, nuclear localization, and the timely release of plasmid DNA following polyplex dissociation for gene transcription. Consequently, the P(S-His)1 derivative of PEI was identified as a potential candidate for use as a gene delivery vector due to its adequate cationic charge, efficient buffering capacity for endosomal escape, minimal toxicity, and enhanced transfection efficiency. Although folic acid conjugation improved cell proliferation, the bulkiness of the PEG group used in the P(S-His)1FP3 polymer as a spacer adversely affected its role as a possible gene delivery agent. Using a low molecular weight PEG group as a spacer between folic acid and the core polymer could be a better option.

Supplementary data

The authors confirm that the supplementary data are available within this article.

Acknowledgements

This work was funded by the Council of Scientific and Industrial Research (CSIR), New Delhi, and the Department of Science & Technology, Government of India, through the project "Facility for Nano/Microparticles-Based Biomaterials-Advanced Drug Delivery Systems" (Grant Number: #8013), under the Drugs & Pharmaceuticals Research Program. We would like to express our gratitude to Dr. T.V. Anilkumar (SCTIMST, Thiruvananthapuram) for his assistance with confocal microscopy, Mr. Willi Paul (SCTIMST) for AFM analysis, Dr. Annie John (SCTIMST) for TEM studies, Dr. Lissy K. Krishnan for providing FACS facilities, and Dr. H.K. Varma for the FTIR facility. We also thank the Director and Head of SCTIMST, Thiruvananthapuram, for providing the necessary facilities.

Conflicts of Interests

The authors declare no conflicts of interest.

Ethical statement

This study did not involve any animal experiments or human subjects.

Authors' contribution

Conceptualization, V.B.M. and C.P.S.; methodology, V.B.M.; software, V.B.M.; validation, V.B.M. and C.P.S.; formal analysis, V.B.M.; investigation, V.B.M.; resources, C.P.S.; data curation, V.B.M. and C.P.S.; writing—original draft preparation, V.B.M.; writing—review and editing, V.B.M. and C.P.S.; visualization, V.B.M. and C.P.S.; supervision, C.P.S.; project administration, V.B.M.; funding acquisition, C.P.S. All authors have read and agreed to the published version of the manuscript.

References

[1] Chang KL, Higuchi Y, Kawakami S, Yamashita F, Hashida M. Efficient gene transfection by histidine-modified chitosan through enhancement of endosomal escape. *Bioconjug. Chem.* 2010, 21(6):1087–1095.

[2] Hashemi M, Parhiz BH, Hatefi A, Ramezani M. Modified polyethyleneimine with histidine-lysine short peptides as gene carrier. *Cancer Gene Ther.* 2011, 18(1):12–19.

[3] Bertrand E, Goncalves C, Billiet L, Gomez JP, Pichon C, *et al.* Histidinylated linear PEI: a new efficient non-toxic polymer for gene transfer. *Chem. Commun. (Camb.)* 2011, 47(46):12547–12549.

[4] Morris VB, Sharma CP. Folate mediated histidine derivative of quaternised chitosan as a gene delivery vector. *Int. J. Pharm.* 2010, 389(1–2):176–185.

[5] Kichler A, Sabourault N, Decor R, Leborgne C, Schmutz M, *et al.* Preparation and evaluation of a new class of gene transfer reagents: poly(-alkylaminosiloxanes). *J. Control. Release.* 2003, 93(3):403–414.

[6] Lu S, Morris VB, Labhasetwar V. Codelivery of DNA and siRNA via arginine-rich PEI-based polyplexes. *Mol. Pharm.* 2015, 12(2):621–629.

[7] Morris VB, Labhasetwar V. Arginine-rich polyplexes for gene delivery to neuronal cells. *Biomaterials* 2015, 60:151–160.
[8] Morris VB, Sharma CP. Enhanced in-vitro transfection and biocompatibility of L-arginine modified oligo (-alkylaminosiloxanes)-graft-polyethylenimine. *Biomaterials* 2010, 31(33):8759–8769.
[9] Morris VB, Sharma CP. Folate mediated l-arginine modified oligo (alkylaminosiloxane) graft poly (ethyleneimine) for tumor targeted gene delivery. *Biomaterials* 2011, 32(11):3030–3041.
[10] Nouri F, Sadeghpour H, Heidari R, Dehshahri A. Preparation, characterization, and transfection efficiency of low molecular weight polyethylenimine-based nanoparticles for delivery of the plasmid encoding CD200 gene. *Int. J. Nanomedicine* 2017, 12:5557–5569.
[11] Shi J, Schellinger JG, Johnson RN, Choi JL, Chou B, *et al.* Influence of histidine incorporation on buffer capacity and gene transfection efficiency of HPMA-co-oligolysine brush polymers. *Biomacromolecules* 2013, 14(6):1961–1970.
[12] Wang DA, Narang AS, Kotb M, Gaber AO, Miller DD, *et al.* Novel branched poly(ethylenimine)-cholesterol water-soluble lipopolymers for gene delivery. *Biomacromolecules* 2002, 3(6):1197–1207.
[13] Yu Y, Wang J, Kaul SC, Wadhwa R, Miyako E. Folic Acid Receptor-Mediated Targeting Enhances the Cytotoxicity, Efficacy, and Selectivity of Withania somnifera Leaf Extract: In vitro and in vivo Evidence. *Front Oncol* 2019, 9:602.
[14] Young O, Ngo N, Lin L, Stanbery L, Creeden JF, *et al.* Folate Receptor as a Biomarker and Therapeutic Target in Solid Tumors. *Curr. Probl. Cancer* 2023, 47(1):100917.
[15] Boogerd LS, Boonstra MC, Beck AJ, Charehbili A, Hoogstins CE, *et al.* Concordance of folate receptor-alpha expression between biopsy, primary tumor and metastasis in breast cancer and lung cancer patients. *Oncotarget* 2016, 7(14):17442–17454.
[16] Schnoell J, Jank BJ, Kadletz-Wanke L, Stoiber S, Gurnhofer E, *et al.* Protein Expression of Folate Receptor Alpha in Adenoid Cystic Carcinoma of the Head and Neck. *Onco Targets Ther.* 2022, 15:531–538.
[17] Ahmadi M, Ritter CA, von Woedtke T, Bekeschus S, Wende K. Package delivered: folate receptor-mediated transporters in cancer therapy and diagnosis. *Chem. Sci.* 2024, 15(6):1966–2006.
[18] Rosenholm JM, Meinander A, Peuhu E, Niemi R, Eriksson JE, *et al.* Targeting of porous hybrid silica nanoparticles to cancer cells. *ACS Nano.* 2009, 3(1):197–206.
[19] Park EK, Kim SY, Lee SB, Lee YM. Folate-conjugated methoxy poly (ethylene glycol)/poly(epsilon-caprolactone) amphiphilic block copolymeric micelles for tumor-targeted drug delivery. *J. Control. Release.* 2005, 109(1–3):158–168.
[20] Benns JM, Mahato RI, Kim SW. Optimization of factors influencing the transfection efficiency of folate-PEG-folate-graft-polyethylenimine. *J. Control. Release* 2002, 79(1–3):255–269.
[21] Corsi K, Chellat F, Yahia L, Fernandes JC. Mesenchymal stem cells, MG63 and HEK293 transfection using chitosan-DNA nanoparticles. *Biomaterials* 2003, 24(7):1255–1264.
[22] Agarwal A, Unfer R, Mallapragada SK. Novel cationic pentablock copolymers as non-viral vectors for gene therapy. *J. Control Release* 2005, 103(1):245–258.
[23] Kim TI, Baek JU, Yoon JK, Choi JS, Kim K, *et al.* Synthesis and characterization of a novel arginine-grafted dendritic block copolymer for gene delivery and study of its cellular uptake pathway leading to transfection. *Bioconjug. Chem.* 2007, 18(2):309–317.

[24] Tracey SR, Smyth P, Herron UM, Burrows JF, Porter AJ, *et al.* Development of a cationic polyethyleneimine-poly(lactic-co-glycolic acid) nanoparticle system for enhanced intracellular delivery of biologics. *RSC Adv.* 2023, 13(48):33721–33735.
[25] Wang X, Niu D, Hu C, Li P. Polyethyleneimine-Based Nanocarriers for Gene Delivery. *Curr. Pharm. Des.* 2015, 21(42):6140–6156.
[26] Chandrasekaran AR. Nuclease resistance of DNA nanostructures. *Nat. Rev. Chem.* 2021, 5(4):225–239.
[27] Hansen MF, Jensen SO, Fuchtbauer EM, Martensen PM. High folic acid diet enhances tumour growth in PyMT-induced breast cancer. *Br. J. Cancer* 2017, 116(6):752–761.
[28] Hwang SY, Kang YJ, Sung B, Jang JY, Hwang NL, *et al.* Folic acid is necessary for proliferation and differentiation of C2C12 myoblasts. *J. Cell. Physiol.* 2018, 233(2):736–747.
[29] Grandinetti G, Smith AE, Reineke TM. Membrane and nuclear permeabilization by polymeric pDNA vehicles: efficient method for gene delivery or mechanism of cytotoxicity? *Mol. Pharm.* 2012, 9(3):523–538.
[30] Ross NL, Munsell EV, Sabanayagam C, Sullivan MO. Histone-targeted Polyplexes Avoid Endosomal Escape and Enter the Nucleus During Postmitotic Redistribution of ER Membranes. *Mol. Ther. Nucleic Acids* 2015, 4(2):e226.
[31] Ross NL, Sullivan MO. Overexpression of caveolin-1 in inflammatory breast cancer cells enables IBC-specific gene delivery and prodrug conversion using histone-targeted polyplexes. *Biotechnol. Bioeng.* 2016, 113(12):2686–2697.
[32] Winkeljann B, Keul DC, Merkel OM. Engineering poly-and micelleplexes for nucleic acid delivery-A reflection on their endosomal escape. *J. Control. Release* 2023, 353:518–534.
[33] Hillaireau H, Couvreur P. Nanocarriers' entry into the cell: relevance to drug delivery. *Cell. Mol. Life Sci.* 2009, 66(17):2873–2896.
[34] Liu P, Anderson RG. Spatial organization of EGF receptor transmodulation by PDGF. *Biochem. Biophys. Res. Commun.* 1999, 261(3):695–700.
[35] Goncalves C, Mennesson E, Fuchs R, Gorvel JP, Midoux P, *et al.* Macropinocytosis of polyplexes and recycling of plasmid via the clathrin-dependent pathway impair the transfection efficiency of human hepatocarcinoma cells. *Mol. Ther.* 2004, 10(2):373–385.
[36] Wang LH, Rothberg KG, Anderson RG. Mis-assembly of clathrin lattices on endosomes reveals a regulatory switch for coated pit formation. *J. Cell Biol.* 1993, 123(5):1107–1117.
[37] Guo W, Lee RJ. Efficient gene delivery via non-covalent complexes of folic acid and polyethylenimine. *J. Control. Release* 2001, 77(1–2):131–138.